

Long-term optical/infrared variability in the quiescent X-ray transient V404 Cyg

C. Zurita¹, J. Casares², R. I. Hynes^{3,4}, T. Shahbaz², P. A. Charles⁴ and E. P. Pavlenko⁵

¹*Centro de Astronomia e Astrofísica da Universidade de Lisboa, Observatório Astronómico de Lisboa, Tapada da Ajuda 1349-018 Lisboa, Portugal**

²*Instituto de Astrofísica de Canarias, Vía Lactea, E-38200 La Laguna, Tenerife, Canary Islands, Spain*

³*Astronomy Department, University of Texas at Austin, 1 University Station C1400, Austin, Texas 78712; USA*

⁴*Department of Physics and Astronomy, University of Southampton, Southampton SO17 1BJ, UK*

⁵*Crimean Astrophysical Observatory, Ukraine*

Accepted 1988 December 15. Received 1988 December 14; in original form 1988 October 11

ABSTRACT

We present the results of optical and infrared photometry of the quiescent X-ray transient V404 Cyg during the period 1992–2003. The ellipsoidal modulations extracted from the most complete databases (years 1992, 1998 and 2001) show unequal maxima and minima with relative strength varying from year to year although their peak to peak amplitudes remain roughly constant at 0.24 ± 0.01 magnitudes. Fast optical variations superimposed on the secondary star’s double-humped ellipsoidal modulation were detected every year with a mean amplitude of ~ 0.07 mags. We have not found significant changes in the activity during this decade which indicates that this variability is probably not connected to the 1989 outburst. We have found periodicities in the 1998 and 2001 data near the 6 hr quasi-periodicity observed in 1992, although we interpret it as consequence of the appearance of a flare event almost every night. Significant variability is also present in the *I* and near infrared (*J* and *K_s*) bands and this decreases slightly or remains approximately constant at longer wavelengths. A cross correlation analysis shows that both the *R* and *I* emission are simultaneous down to 40 s.

Key words: circumstellar matter – infrared: stars.

1 INTRODUCTION

Low-Mass X-ray Binaries (LMXBs), are semi-detached binary systems where a normal low-mass late type star transfers gas onto a compact remnant i.e. a neutron star or black hole. A significant fraction of LMXBs are soft X-ray transients (SXTs) characterized by episodic X-ray outbursts where the luminosity increases dramatically. During the long intervals (usually many years) between outbursts, the SXTs are in quiescence and the optical emission is dominated by the radiation from the companion star. This offers a superb opportunity to analyze and obtain dynamical information which eventually enables us to constrain the nature of the compact object (see eg. Charles 1998, Casares et al. 2001). The majority of these systems appear to contain black holes and they are, in fact, the best evidence we have for the existence of stellar mass black holes. The most secure case is the SXT V404 Cyg which has a mass function of $6.08 \pm 0.06 M_{\odot}$ (Casares,

Charles & Naylor 1992), twice the usually accepted upper limit to that of a neutron star (Rhoades & Ruffini 1971). The estimated mass for the compact object is $12 \pm 2 M_{\odot}$ (Shahbaz et al. 1994) which, together with GRO 1915+105 (Greiner, Cuby & McCaughrean 2001), are the most massive stellar mass black holes yet measured.

Furthermore, V404 Cyg is considered a peculiar SXT because it has one the longest orbital periods (6.5 d; Casares et al. 1992) and is the most X-ray luminous in quiescence ($L_X \sim 10^{33} - 10^{34} \text{ erg s}^{-1}$; Garcia et al. 2001). Apart from this, it is largely known that V404 Cyg exhibits short-term (sub-orbital) variations during quiescence in the optical continuum (Wagner et al. 1992; Pavlenko et al. 1996) and H α flux (Casares & Charles 1992; Casares et al. 1993) where the H α profiles seems to be correlated to the continuum (Hynes et al. 2002). The infrared (Sanwal et al. 1995), X-rays (Wagner et al. 1994; Kong et al. 2002) and radio (Hjellming et al. 2000) are also variable. Recent simultaneous observations in X-rays and optical show that optical line and continuum variability are well correlated

* E-mail: czurita@oal.ul.pt (CZ)

with X-rays flares (Hynes et al. in preparation). On the other hand it seems that fast variability during quiescence is not a peculiarity of V404 Cyg but a fingerprint of quiescent SXTs, irrespective of the nature of the compact object (Zurita, Casares & Shahbaz 2003; Hynes et al. 2003, hereafter ZCS). Although these variations seem to originate in the accretion disc rather than in the optical companion or gas stream/hot spot (Zurita & Casares 1998; Hynes et al. 2002, ZCS) the underlying physical mechanism is not yet understood. The dynamical (Keplerian) timescales associated with these fluctuations suggest that the flares are produced in the outer disc (ZCS). Alternatively, based on the similarities of the power density spectrum (PDS) of A0620-00 to those of low/hard state sources Hynes et al. (2003) have pointed out that the optical variability is at least partly related to the inner accretion flow even in quiescence. This suggestion was also supported by the discovery of the correlated optical and X-ray flares (Hynes et al. in preparation).

Since V404 Cyg is the brightest SXT, and hence accessible with 1-m type telescopes, we embarked on a study of the fast variability over the period 1992–2003. This paper comprises of a simultaneous optical and infrared photometric study, with the aim to determining the colour of the variability and its possible origin.

2 OBSERVATIONS AND DATA REDUCTION

We obtained CCD photometry of V404 Cyg with various 1-m-class telescopes during the years 1992, 1998, 1999, 2001, 2002 and 2003. The 1992 data were obtained in the Johnson *R* band with the GEC CCD camera on the 1 m JKT telescope at Observatorio del Roque de los Muchachos. V404 Cyg was observed in 1998 simultaneously in the *R* and *I* band with identical Thomson CCD cameras at both the 0.8 m IAC80 and 1 m OGS telescopes at Observatorio del Teide. We also obtained *R* band photometry in 1999 with the SITE2 CCD camera on the JKT. Further details on the 1992 and 1999 observations can be found in Pavlenko et al. (1996) and Hynes et al. (2002) respectively. During Jul–Sep 2001 *R*-band and *J* and *K_s* simultaneous observations were performed using the Thomson CCD camera at the 0.8 m IAC80 and the infrared camera at the 1.5 m *Telescopio Carlos Sánchez* (TCS) also at Observatorio del Teide. Finally we observed V404 Cyg during May–Jun 2002 and Jul 2003 also in the *R*-band and with identical Thomson CCD cameras at both the 0.8 m IAC80 and 1 m OGS telescopes at Observatorio del Teide. Full details of these observations are given in Table 1.

All images were corrected for bias and flat-fielded in the standard way using IRAF. Seeing conditions were not good enough to cleanly separate the contribution of the target and its nearby (1.4 arcsec) line-of-sight star (Udalski & Kaluzny 1991) so we applied straightforward aperture photometry using a large aperture of 3.5 arcsec which adds the flux from both stars and which was subsequently corrected (see next section). Several comparison stars within the field of view were checked for variability during each night and during the entire data set.

3 THE *R* BAND LIGHT CURVES

3.1 The ellipsoidal modulation

The true V404 Cyg *R*-band lightcurves were obtained after subtracting the contribution of the *contaminating* companion star, assuming that it had $R=17.52\pm 0.01$ as given in Casares et al. (1993). We then folded our data using the ephemeris of Casares & Charles (1994). These lightcurves show the classical secondary’s ellipsoidal modulation (see Shahbaz et al. 1994) although with superposed variability.

The ellipsoidal modulation is due to the differing aspects that the tidally distorted secondary star presents to the observer through the orbital cycle. An ideal pure ellipsoidal lightcurve is hence a double humped modulation with two equal maxima and two somewhat different minima (the minimum at phase 0.5 is deeper because gravity darkening is more pronounced in the direction of the L_1 point (Avni & Bahcall 1975). This modulation was first simulated employing two sine waves at the orbital frequency and its first harmonic, where the fundamental allows the minima to vary. Relative phases were fixed to produce equal maxima. However, it has been largely reported that lightcurves of quiescent transients often exhibit unequal maxima as well (eg. A0620-00: Haswell 1996; Gelino, Harrison & Orosz 2001- J1118+480: Zurita et al. 2002- J2123-058: Shahbaz et al. 2003). The distortions from the theoretical case could be explained assuming a non-constant contribution of the accretion disc, X-ray heating, spots on the surface of the secondary star or light from the stream impact point. In any case, we also account for this possibility by allowing the sine phases to vary independently. We then fitted these two models to the mean light curve and also to the lower envelope. The lower envelope was constructed as has been previously explained in Pavlenko et al. (1996) and ZCS, that is, for each night we have selected all brightness estimates which differ from the minimum by no more than twice the accuracy of the observations. The selected data were then averaged in time and phase intervals. We found the best representation (the minimum χ^2) fitting the lower envelope with the second model. These fits for the years with a most complete database (1992, 1998 and 2001) are shown in Figure 1. Both minimum and maximum magnitudes varies. The maximum at phase 0.25 is higher than at phase 0.75 and also the minimum at phase 0.5 is deeper than at phase 0. However their relative strength changes from year to year. Apart from this, the peak to peak amplitude of the first harmonic remains roughly constant at 0.24 ± 0.01 magnitudes, a key fact in the modeling of V404 Cyg and the determination of its component masses. We note that the 1998 lightcurve obtained by Pavlenko et al. (2001) in the same band exhibits equal maxima, however we cannot conclude whether this behaviour reflects a real change in the system, since both lightcurves are not simultaneous, or is due to an incomplete sampling.

3.2 The superimposed fast variability

We assumed that the fast variability superimposed on the ellipsoidal curve is not related to the ellipsoidal modulation so the former was isolated by subtracting the lower envelope

Table 1. Log of observations

<i>Night</i>	<i>Band</i>	<i>Resolution (s)</i>	<i>Monitoring time (hr)</i>
1992			
1 m JKT			
Jun 27	<i>R</i>	259	1.45
Jun 28	<i>R</i>	259	5.44
Jun 29	<i>R</i>	259	2.51
Jun 30	<i>R</i>	259	7.11
Jul 1	<i>R</i>	259	7.07
Jul 2	<i>R</i>	259	5.33
Jul 3	<i>R</i>	259	6.18
Jul 4	<i>R</i>	259	5.15
Jul 5	<i>R</i>	259	4.11
Jul 6	<i>R</i>	259	6.16
Jul 7	<i>R</i>	259	6.37
Jul 8	<i>R</i>	259	6.10
Jul 9	<i>R</i>	259	7.24
Jul 10	<i>R</i>	259	5.67
Jul 11	<i>R</i>	259	6.68
Jul 12	<i>R</i>	259	6.29
1998			
0.8 m IAC80 / 1 m OGS			
17 Aug	<i>R</i>	94	3.98
18 Aug	<i>R</i>	88	6.09
19 Aug	<i>R</i>	79	6.32
21 Aug	<i>R / I</i>	129 / 99	6.52 / 7.38
22 Aug	<i>R / I</i>	146 / 99	6.21 / 5.88
23 Aug	<i>R / I</i>	136 / 129	6.77 / 1.08
24 Aug	<i>R / I</i>	136 / 129	7.03 / 7.28
25 Aug	<i>R / I</i>	138 / 129	6.74 / 7.21
26 Aug	<i>R</i>	136	4.54
27 Aug	<i>R</i>	136	7.19
1999			
1 m JKT			
Jul 6	<i>R</i>	80	5.89
Jul 7	<i>R</i>	80	6.05
2001			
0.8 m IAC80 / 1 m TCS			
31 Jul 01	<i>R</i>	314	3.80
1 Aug	<i>R</i>	314	4.12
2 Aug	<i>R</i>	314	5.22
3 Aug	<i>R / J / K_s</i>	314 / 1062 / 1100	4.98 / 4.80 / 2.56
4 Aug	<i>R</i>	314	4.17
6 Aug	<i>R / J / K_s</i>	314 / 1054 / 1100	3.88 / 1.80 / 3.72
7 Aug	<i>R / J / K_s</i>	314 / 1030 / 1040	3.37 / 3.05 / 2.73
8 Aug	<i>R / J / K_s</i>	314 / 1030 / 1050	4.04 / 2.53 / 3.83
10 Aug1	<i>R / J / K_s</i>	314 / 1630 / 1050	4.34 / 4.44 / 3.53
11 Aug1	<i>R</i>	197	3.87
28 Aug1	<i>R / J / K_s</i>	314 / 1100 / 1050	5.19 / 5.32 / 5.05
30 Aug1	<i>R / J / K_s</i>	314 / 1150 / 1050	5.94 / 5.36 / 5.04
31 Aug1	<i>R</i>	314	6.54
6 Sep	<i>R</i>	314	3.84
8 Sep	<i>R</i>	314	4.78

variable-phase sinusoidal fit (as has been explained in the previous subsection) from the original data resulting in a light curve essentially free from the ellipsoidal modulation. In the case of the 1999 lightcurve, because only two nights of observations were available, we fixed all the parameters of the double sine wave obtained from the 1998 fit except the phase of the first sine. In 2003 only five nights of observations are available so we fixed the mean magnitude in the variable-phase fit at the value we obtained with

the simplest constant relative phase fit. Furthermore, in order to compare the results from different years, we have resampled the lightcurves to have the same temporal resolution (320s). The lightcurves and the corresponding lower envelope fits are shown in Figure 2 and the result of the subtraction is represented in Figure 3.

Examining these lightcurves we find that the observed variations resemble the lightcurves of stellar flares, i.e. rapid

Table 1. Log of observations (continuation)

<i>Night</i>	<i>Band</i>	<i>Resolution (s)</i>	<i>Monitoring time (hr)</i>
2002:			
1 m OGS			
27 May 02	<i>R</i>	315	4.02
28 May 02	<i>R</i>	315	3.90
02 Jun 02	<i>R</i>	315	4.27
03 Jun 02	<i>R</i>	315	4.42
0.8 m IAC80			
01 Jun 02	<i>R</i>	315	3.37
04 Jun 02	<i>R</i>	315	2.05
2003:			
1 m OGS			
17 Jul 03	<i>R</i>	252	1.20
18 Jul 03	<i>R</i>	252	8.20
19 Jul 03	<i>R</i>	252	4.33
20 Jul 03	<i>R</i>	252	8.26
0.8 m IAC80			
28 Jul 03	<i>R</i>	352	8.72

and strong increases in brightness. We consider a *flare* to be any variation which differs from the mean level by more than 3σ . We found in many nights large single events of ~ 2 h or more duration appearing together with faster and small amplitude variations. Other nights, however, only the faster variations are present. The shape of the large flares seem to be symmetric with similar rise and decay times. In order to characterize the flares and quantify the flare activity we calculate the mean, \bar{z} , standard deviation corrected for the instrumental error, σ_z (i.e. we subtract the instrumental error in quadrature) and *equivalent duration* (Π_z) of the relative intensity lightcurves, i.e. relative to the steady non-variable level (see ZCS).

Here z is the *relative intensity*, defined as:

$$z = (I - I_q)/I_q \quad (1)$$

where I and I_q are the observed intensities of the flaring and not flaring state respectively.

The equivalent duration (Π) is defined as:

$$\Pi = \int z dt \quad (2)$$

The total energy of the flare (E) is obtained by multiplying the equivalent duration by the system's luminosity. i.e. $E = 4\pi d^2 F_q \Pi$ erg (where d is the distance to the system and F_q is the dereddened observed quiescent flux). The time-averaged flare luminosity $\langle L_R \rangle$ is defined as the sum of the energies of the individual flares divided by the total monitoring time (M_t). The system properties and the resulting parameters of the variability are summarized in Tables 2 and 3 respectively.

We note that the flare mean level and the time-averaged flare luminosity are somewhat sensitive to the ellipsoidal model which is subtracted. It may be that the model is not an ideal representation of the non-variable level due to our incomplete sampling and effects other than the flares which distort the ellipsoidal modulation. In contrast, the standard deviation (σ_z) is not significantly affected by the model assumed. We hence consider that σ_z is the best flare

level activity indicator. We do not find any clear trend towards increasing or diminishing flare activity with time (see Table 3 and Fig. 4). Moreover, the long-term photometric study of V404 Cyg during quiescence performed by Pavlenko et al. (2001) also shows the fast variability persisting over the decade 1992-2000 with variable amplitude. In particular in 2000 the mean amplitude was 0.06. This is consistent with our data as is clear in Fig. 4. We estimate the flare activity to be roughly constant with $\bar{z} \sim 0.065$, $\sigma_z \sim 0.036$ and $\langle L_R \rangle \sim 13 \times 10^{32}$ erg s $^{-1}$. Assuming that the X-ray (0.3-7 keV) luminosity is $\langle L_X \rangle \sim 5 \times 10^{33}$ erg s $^{-1}$ (from the Chandra spectrum; Kong et al. 2002) we estimated the ratio between optical flare and X-rays luminosities: $\langle L_{opt}/L_X \rangle \sim 0.3$

4 SEARCHING FOR PERIODICITIES

As the short term variations are non-sinusoidal we have attempted to analyze and separate the periodicities present in the data by fitting a Fourier series to the lightcurves over a range of frequencies, ν (Martinez & Koen 1994). A plot of the reduced χ^2 of each fit versus ν should have a minimum at the fundamental frequency of oscillation in the data.

We applied this method after resampling the data from different years to the same time resolution, and after detrending the long-term variations by subtracting the lower envelope as explained in the previous section. We rejected those nights having less than 3 hrs coverage so as to avoid peculiar offsets due to poor sampling. The χ^2 spectrum is computed in the range 3 to 10 cycles d $^{-1}$ with a resolution of 5×10^{-2} cycles d $^{-1}$ and with 3 terms in the Fourier series. They are shown in Fig. 5 where we have also marked the 68 percent confidence limit at $\chi_{min}^2 + 1$ (e.g., Lampton, Margon & Bowyer 1976)

With the 1992 data, we reproduce the results already published in Pavlenko et al. (1996). There exist a peak in the vicinity of 6 hr (0 d .25) which is split into two (at

Table 2. V404 Cyg properties.

<i>Distance (kpc)</i>	3.5±0.2
<i>A_V</i>	4.0
<i>Spectral Type</i>	K0IV
<i>inclination</i>	56°±2
<i>P_{orb} (days)</i>	6.64714
<i>Derreddened magnitudes</i>	R=13.5, I=13.81, J=12.55, K=12.05

Parameters extracted from Wagner et al. (1992); Shahbaz et al. (1994); Pavlenko et al. (1996); Martin (1999) and Casares et al. (1993).

Table 3. V404 Cyg flares properties for the different years.

<i>Year</i>	$\langle \Pi^\dagger \rangle$	<i>Monitoring time (hr)</i>	$\langle L_R \rangle$ $\times 10^{32} \text{ erg s}^{-1}$	\bar{z}_f	σ_z
1992	0.055	88.9	10.7±0.4	0.057	0.040
1998	0.084	61.4	15.8±0.5	0.084	0.034
1999	0.066	11.9	12.5±0.4	0.067	0.025
2001	0.065	68.1	12.7±0.4	0.061	0.042
2002	0.071	22.0	15.1±0.5	0.064	0.038
2003	0.073	30.7	13.8±0.5	0.067	0.041

(†) Time averaged equivalent duration of the individual flares divided by the total monitoring time.

0^d.260 and 0^d.246) with a central peak coinciding with the median value of these periods (at 0^d.253). The 1 day aliases are also visible. A detailed analysis of these data can be found in Pavlenko et al. (1996). The 1998 spectrum shows two peaks at 0^d.247 and 0^d.233 exceeding the 68 percent confidence interval and also their 1 day aliases. The power spectrum of the 2001 data is very noisy and we found two possible periods at 0^d.241 and 0^d.235 (also with their aliases) and two other peaks at 0^d.261 and 0^d.250 all of them with the same significance. We note that these data were also analysed in ZCS. Here a Lomb-Scargle periodogram was performed yielding significant peaks only above 1 hour but with a complicated alias pattern which makes it difficult to distinguish any periodicity. Finally, we also note that Hynes et al. (2002) analysis of the 1999 lightcurves obtained at CrAO and SAI¹ together with our 1999 JKT data could not find any clear periodicity. Here the peak with highest significance has a period of 0^d.254 although other periods are also possible. Clearly there is no coherent period in our database but variability on a characteristic timescale of about 6 hours is detected.

5 THE COLOUR OF THE FLARES

5.1 The 1998 simultaneous *R* and *I* photometry

V404 Cyg was also observed simultaneously in the *R* and *I* bands during 1998. To extract the true *I* magnitudes of V404 Cyg, we previously subtracted the contribution of the *contaminating* star, *I_{cs}*. We calibrated the unresolved pair of V404 Cyg plus contaminating star using the *I*

magnitudes tabulated in Martin (1999) and then subtracted the real median magnitude of V404 to find $I_{cs} = 17.0 \pm 0.1$. The resulting lightcurve is shown in figure 6, where fast variability is clearly superimposed on the ellipsoidal modulation. We detrended the long-term ellipsoidal modulation by subtracting the lower envelope as explained in section 3. We also binned the lightcurves to 300 s.

Variability is clearly seen in the *I* band as well, following the same pattern as the variability in the *R* band (see Fig. 8). We calculate the mean, standard deviation of the lightcurves and the equivalent duration of the flares relative to the steady non-variable level in both the *R* and *I* bands. We note that although the time resolution is the same, the parameters for the *R* band change from those reported in section 6 since now we are only including in our analysis the nights with simultaneous observations. The results are given in table 4.

The flare activity in the *R* band is larger than in the *I* band although we note that the relative contribution of the secondary star and the accretion disc to the total light is different at both wavelengths. In the case of V404 Cyg the distribution of the veiling rises toward the blue following a power law of index $\alpha = -3.4 \pm 0.9$ which basically reflects the drop in the photospheric flux of the last-type companion short ward of 5300 Å (Casares et al. 1993). We also calculated the fluxes of the flares in both bands. To do it we first de-redden the observed magnitudes using for the reddening a value of $A_V = 2.8$ (see Shahbaz et al. 2003b) and then subtracted the ellipsoidal modulation constructed as explained in the previous sections from the de-reddened lightcurve yielding the monochromatic flux of the flares. We obtained $F_R = 1.25 \text{ mJy}$ and $F_I = 0.41 \text{ mJy}$, so the mean flux density ratio of the flares is $F_R/F_I \sim 3$. Nevertheless there exists several sources of error in the calculation of the

¹ with the 0.38-m telescope of the Crimean Astrophysical Observatory (CrAO) and the 1.25- and 0.6-m telescopes of the Sternberg Astronomical Institute (SAI) in 1999.

Table 4. V404 Cyg flares properties for the *R* and *I* bands in 1998.

<i>Band</i>	$\langle \Pi^\dagger \rangle$	<i>Monitoring time (hr)</i>	$\langle L \rangle$ $\times 10^{32} \text{ erg s}^{-1}$	\bar{z}_f	σ_z
R	0.097	28.8	18.2±0.6	0.095	0.030
I	0.038	28.8	3.8±0.1	0.039	0.019

(†) Time averaged equivalent duration of the individual flares divided by the total monitoring time.

flare fluxes. First, there is the photometric errors as well as the correction of the flux from the nearby star which contaminates V404 Cyg (see section 3). The photometric accuracy is ~ 1 percent in both bands but the magnitude of the contaminating star is known with a $\sim 1\%$ and $\sim 10\%$ accuracy in *R* and *I* respectively although, in fact, we must consider these values as lower limits since they were obtained from the literature and there is difference between effective band passes on different telescopes. But the main source of error is the determination of the reddening. If we use the extreme values for the reddening $A_V=4.0$ and $A_V=2.2$ (Casares et al. 1993; Shahbaz et al. 1994) we found an 80% error in the determination of the ratio F_R/F_I . In addition we should note that the lower envelope could not reproduce accurately the secondary's star lightcurve since there are several factors which distort the ellipsoidal modulation that we cannot quantify.

To test if the flaring activity is simultaneous in the two bands, or if one lags the other, we calculated cross-correlation functions between them. This analysis identifies correlations and reveals the mean lag between the *R* and *I* variability. We used the Discrete Correlation Function or *DCF* (Edelson & Krolik 1988). Our *DCF*, for the nights when simultaneous observations last more than 6 hours (21, 24 and 25 Aug.), is shown in figure 7. Here positive lags correspond to *R* variations lagging behind those in *I*. The correlation is clearly significant at the 3σ level although the peak appears asymmetric. This could correspond to *R* variations lasting longer than those in *I*. According to Tonry & Davis (1979), we estimate a delay of *R* with respect to *I* of (49 ± 40) s. The measured delay is clearly not significant at the 3σ level and is below the time resolution used, so is almost certainly not real. We hence conclude that both the *R* and *I* emission are simultaneous within the observational errors. In fact this is the result we expect since both bands are close in wavelength and so probably originate in the same region.

5.2 The 2001 simultaneous *R* and infrared photometry

Because the fractional quiescent emission rises toward the infrared, it is of considerable interest to investigate the properties of the flare emission in this band. Even in the infrared the remaining contamination due to flares can have significant impact on the binary parameters derived from modeling the ellipsoidal variations (e.g. Sanwal et al. 1995; Shahbaz et al. 1996). We also observed V404 Cyg simultaneously at optical and infrared wavelengths during 2001. After performing aperture photometry around the target and its close companion, we subtracted the latter by assuming $J=14.53$ (Casares et al. 1993) and $K=14.3$

(Shahbaz et al. 1996). The lightcurve is shown in figure 9, where fast variability is superimposed on the ellipsoidal modulation.

We removed the long-term ellipsoidal modulation by again subtracting the lower envelope as in section 3. The non-ellipsoidal variability is shown in figure 11. To obtain the same temporal resolution in all filters, we first binned the *R* data and then performed linear interpolation of the *R* and K_s magnitudes to the times when the *J* magnitudes are given. We note variability above the noise level, also in the infrared bands. In some nights the infrared emission is clearly correlated with the optical (7, 8, 10 and 28 Aug.), with amplitudes $\Delta J \sim 0.16$ mags and $\Delta K_s \sim 0.08$ mags. On the night of 3 Aug. the K_s flux shows a steep variation with 0.1 mags amplitude and ~ 1 hour duration not correlated with the optical or *J* band flux.

In this case we also obtained the flux densities as was made in the previous section using the extinction law by Rieke & Lebofsky (1985). These fluxes in the regions with simultaneous photometry are $F_R=0.97$ mJy, $F_J=0.68$ mJy and $F_K=0.23$ mJy. Assuming $F_R/F_I \sim 3$ and a ~ 80 percent uncertainty in this ratio (see previous section) we estimated the flux density in the *I* band. Also we compared our values with those obtained by Shahbaz et al. (2003b) to extract the spectrum of the flares (Fig 10). These last values are actually the fluxes at the peak of individual flares so we consider them as upper limits. Apart from this, we can only obtain a very rough estimation since we are comparing data from different epochs and with large uncertainties.

In order to characterize the flare activity, we calculate the parameters of the variability in the three bands, the results being given in table 5. We found lower activity at longer wavelengths although, as we will discuss in the next section, the relative contribution of the accretion disc depends on the waveband and hence a further correction must to be made.

6 DISCUSSION

Our *R* band lightcurves, obtained during the period 1992-2003, show considerable suborbital variability in addition to the ellipsoidal modulation. Assuming that these variations are not connected, we obtained a representation of the ellipsoidal modulation of the tidally distorted secondary star by fitting a double sine to the lower envelope of the lightcurve. The fits performed with the most complete

Table 5. Flares properties for optical and infrared in 2001.

<i>Band</i>	$\langle \Pi^\dagger \rangle$	<i>Monitoring time (hr)</i>	$\langle L \rangle \times 10^{32} \text{ erg s}^{-1}$	\bar{z}_f	σ_z
R	0.071	21.1	13.5±0.4	0.069	0.036
J	0.057	21.1	7.7±0.3	0.058	0.029
K	0.035	21.1	1.8±0.1	0.029	0.012

(†) Time averaged equivalent duration of the individual flares divided by the total monitoring time.

databases (years 1992, 1998 and 2001) show unequal maxima and minima with relative strength varying from year to year. This behavior could be explained assuming starspots on the secondary star. This is a very widespread phenomenon among cool stars. Axial rotation of a spotted star and slow variations of the starspot geometry cause photometric variability which is expressed in brightness rotational modulation and slow variations of mean stellar lightcurves. Other possibility is they are produced by changes in the accretion disc geometry and brightness due a superhump, i.e. optical modulation as a consequence of the precession of an eccentric accretion disc by perturbation from the secondary. This is a very promising suggestion since superhumps in a quiescent SXT have already been detected (J1118+480, Zurita et al. 2002). Superhumps have also been largely invoked to explain the changing quiescent lightcurve of the prototypical black hole candidate: A0620-00 (eg. Haswell 1996). After subtracting the corresponding lower envelope fits from the original data the lightcurves are dominated by large flares ($\sim 0^m.2$) lasting a few hours. In addition, shorter timescale variability ($\sim 0^m.05$) is present with lower amplitude. Our photometry indicates that the flaring activity did not change significantly over this 10-year interval which indicates that this variability is probably not connected to the 1989 outburst.

We have also found significant variability in the *I* and near-IR band (*J* and *K_s*) and these are correlated. In 1990, just one year after the outburst, a variation of $\sim 0^m.2$ was seen in several visible bands (Casares et al. 1993). In 1991, the variability originally interpreted as a six hour modulation, decreased to $\sim 0^m.1$, but no significant changes were reported in the interval 1992-1993 (Martin 1999). Infrared photometry in 1990, was dominated by a $\sim 0^m.2$ amplitude at a periodicity of ~ 6 hours (Casares et al. 1993). Also 1993 *H* band data presents significant variability contaminating the ellipsoidal modulation (Sanwal et al. 1995). They reported an *rms* scatter of $\sim 0^m.04$ for V404 Cyg and $\sim 0^m.02$ for the comparison star. This yields a flare activity level of $\sigma_z \sim 0.032$, which is consistent with our values. In 1993, *K* band photometry obtained by Shahbaz et al. (1994) does not show short term variability, with an upper limit of $\sim 0^m.03$. However in this case, only one night of more than 6 hours of continuous coverage was obtained.

We have also found that lower activity is found at longer wavelengths. However, as we have pointed out in ZCS the flare activity level calculated as σ_z represents the flare activity relative to the underlying smooth modulation (F_q). F_q contains two distinct components: the flux from the companion star, F_c and the flux from the non-variable, steady

accretion disc, F_d (see figure 9 in ZCS for clarity). The relative contribution of the accretion disc depends on the wave band and hence, if we assume that the flares are produced in the accretion disc (see Hynes et al. 2002, ZCS), a more useful parameter to compute is the flare activity relative to the flux from the steady disc, rather than relative to the total non-variable flux, which is given by

$$\sigma_z^* = \sigma_z / \eta_d \quad (3)$$

where

$$\eta_d = F_d / F_q = (1 + F_c / F_d)^{-1} \quad (4)$$

We can determine η_d using the spectroscopic value for the veiling η_{obs} , which is defined as

$$\eta_{\text{obs}} = \frac{\bar{F}_f + F_d}{\bar{F}_f + F_q} \quad (5)$$

where \bar{F}_f is the mean flux of the flares, and find

$$\eta_d = (\bar{z}_f + 1) \eta_{\text{obs}} - \bar{z}_f \quad (6)$$

Casares et al. (1993) reported that the accretion disc contributes 11-16 percent of the observed flux in *R* (see also Casares & Charles (1994)). Therefore we assume an observational veiling of $\eta_{\text{obs}} = 13\%$ in this band. We also estimate an observational veiling of $\sim 12\%$ in the *I* band by extrapolating from the veiling in *B*, *V* and *R* (Casares et al. 1993). On the other hand, Shahbaz et al. (1996) determined the fraction of the light arising from the accretion disc in the *K* band varies from 0 to an upper limit of 11 percent. We hence consider $\eta_{\text{obs}} = 5$ percent in this case. The corrected values using these factors, are tabulated in table 6. The uncertainties on the veiling and the limited database only allows us to say that the activity diminishes slowly or remains approximately constant through the IR. In the 1992 series of *B*, *V*, *R* and *I* band observations (16 measurements spread over 16 nights; see Martin 1999) an estimate of the variability could be obtained by comparing the variance with the photometric noise and the optical variations. This variance increases toward the blue suggesting that the source of fast variability in V404 is indeed blue. We note however that Shahbaz et al. (2003b) determined the colour of the large flares and found the *i'* ($\lambda_{\text{eff}} 7650\text{\AA}$) band flux to be larger than that in the *g'* ($\lambda_{\text{eff}} 4750\text{\AA}$) band. Comparing with these data we obtained an estimated spectrum with a peak at $\lambda_{\text{eff}} 7000\text{\AA}$ (see Fig. 10).

In an attempt to compare the infrared variability we also observed the SXT with highest flares: J0422+32, where events as high as 0.6 mag were observed (ZCS). Observations of this system in the *H* band covering half of its orbital period do not show variability above ~ 0.06 mags,

Table 6. Flare activity and veiling factors for *R*, *I* and *K* band.

<i>Band</i>	η_{obs} (percent)	η_{d} (percent)	\bar{z}_f	σ_z	σ_z^*
R	13	14.1	0.095	0.030	2.1×10^{-3}
I	12	12.4	0.039	0.019	1.5×10^{-3}
R	13	13.8	0.069	0.036	2.6×10^{-3}
K	5	5.1	0.029	0.012	2.3×10^{-3}

the estimated error of our photometry (Zurita et al. in preparation). Comparing with the variability we observed in the *R'* band (ZCS) and assuming that the disc contributes $\sim 30\%$ in *H* (Beekman et al. 1997) we estimate that the activity in the infrared is, at least, 33% lower than in the optical. Although only a very crude estimation can be made, among other things because the observations are not simultaneous and because the value of the veiling is not well determined, it seems that the spectrum of J0422+32 flares also drop at longer wavelengths. On the other hand, no significant contamination of the infrared lightcurves of J0422+32 has been found by Gelino & Harrison (2003).

The quasi periodic oscillations noticed in the earliest data (1992 - see Pavlenko et al. 1996) are less clear in our more recent data (1998 and 2001). However, the periodograms show peaks close to 6 hr at the 68 percent significance level which could be interpreted as a consequence of the appearance of a flare event almost every night. Shahbaz et al. (2003) found a *QPO* feature at 21.5 minutes attributed to variability at the *ADAF* transition radius. Our longer sampling does not allow us to test this hypothesis. It is possible in any case that variability with different timescales have different origin.

ACKNOWLEDGMENTS

CZ acknowledges support from the Fundação para a Ciência e a Tecnologia, Portugal. IH acknowledges support from grant F/00-180/A from the Leverhulme Trust and through Hubble Fellowship grant #HF-01150.01-A awarded by the Space Telescope Science Institute, which is operated by the Association of Universities for Research in Astronomy, Inc., for NASA, under contract NAS 5-26555. TS acknowledges support from the Spanish Ministry of Science and Technology under project AYA 2002 03570.

REFERENCES

- Avni Y., Bahcall J.N., 1975, *ApJ*, 197, 675
Casares J., Charles P.A., 1992, *MNRAS*, 255, 7
Casares J., Charles P.A., Naylor T., 1992, *Nature*, 355, 614
Casares J., Charles P.A., Naylor T., Pavlenko E.P., 1993, *MNRAS*, 265, 834
Casares J., Charles P.A., 1994, *MNRAS*, 271, L5
Casares J., 2001, in F. C. Lázaro, M. J. Arévalo, eds, *Lecture notes in physics* Vol. 563, *Binary stars: selected topics on observations and physical processes*. Springer, Berlin, p. 277
Charles P.A., 1998, In: 'Theory of black hole accretion discs', M.A. Abramowicz, G. Björnsson, J.E. Pringle (Eds), Cambridge Contemporary Astrophysics, Cambridge University Press, p.1
Edelson R.A., Krolik J.H., 1987, *ApJS*, 65, 1
Garcia M.R., McClintock, J.E., Murray S.S., Callanan P.J., Narayan R., 2000, Poster presented at 2000 HEAD Meeting
Garcia M.R., McClintock, J.E., Narayan R., Callanan P., Murray S.S., 2001, *ApJ*, 533, L47
Gelino D.M., Harrison T.E, Orosz J.A, 2001, *AJ*, 122, 2668
Gelino D.M., Harrison T.E, 2003, astro-ph/0308490
Gershberg R.E., 1972, *ApSS*, 19, 75
Greiner J., Cuby J.G., McCaughrean M.J., 2001, *Nature*, 414, 522
Gurzadyan G.A., 1980, *International Series in Natural Philosophy*, Oxford: Pergamon Press, 1980, Rev. ed.
Gurzadyan G.A., 1988, 332, 183
Haswell C.A., 1996, in *proc. IAU Symp. 165: Compact Stars in Binaries*, Eds. J. van Paradijs, E.E.J., van der Heuvel, E. Kuulkers, Kluwer Academic Publishers, Dordrecht, p351
Haisch B., Strong K.T., Rodono M., 1991, *ARA&A*, 29,275
Henoux J.C., Abouadarham J., Brown J.C., van den Oord G.H.J., van Driel-Gesztelyi L., 1990, *A&A*, 233, 577
Hjellming R.M., Rupen M.P., Mioduszewski A.J., Narayan R., 2000, *ATel*, 54,1
Hynes R.I., Zurita C., Haswell C.A., Casares J., Charles P.A., Pavlenko E.P., Shugarov S.Y, Lott D.A., 2002, *MNRAS*, 330, 1009
Hynes R.I., Charles P.A., Casares J., Haswell C.A., Zurita C., Shahbaz T., 2003, *MNRAS*, 340, 447
Kong A.K., McClintock J.E., Garcia M.M., Murray S.S., Barret D., 2002, *ApJ*, 570, 277
Lampton M., Margon B., Bowyer S., 1976, *ApJ*, 208, 177
Lu E.T., Hamilton R.J., 1991, *ApJ*, 380, 89
Martin A.C., Ph.D. Thesis, 1999, Oxford Univ., Oxford
Martinez P., Koen C., 1994, *MNRAS*, 267, 1039
Pavlenko E.P., Martin A.C., Casares J., Charles P.A., Ketsaris N.A., 1996, *MNRAS*, 281, 1094
Pavlenko E.P., Kuznetsova Y.G., Shugarov S. Yu, Petrov V.S., 2001, *ApSSS*, 276, 65
Rhoades C.E., Ruffini R., 1971, *ApJL*, 163, L83
Rieke G.H., Lebofsky M.J, 1985, *ApJ*, 288, 618
Sanwal D., Robinson E.L., Zhang E., Colomé C., Harvey P.M., Ramseyer T.F., Hellier C., Wood, J.H., 1995, *ApJ*, 460, 437
Shahbaz T., Ringwald F.A., Bunn F.A., Naylor T., 1994, *MNRAS*, 271, L10
Shahbaz T., Bandyopadhyay R., Charles P.A., Naylor T., 1996, *MNRAS*, 282, 977

Shahbaz T., Zurita C., Casares J., Dubus G., Charles P.A.,
 Wagner R. Mark, Ryan E., 2003, MNRAS, 585, 443
 Shahbaz T. et al., astro-ph/0309648
 Tonry J., Davis M., 1979, AJ, 84, 1511
 Udalski A., Kaluzny J., 1991, PASP, 103, 198
 Wagner R.M., Kreidl T.J., Howell S.B., Starrfield S.G.,
 1992, 401, L97
 Wagner R.M., Starrfield S.G., Hjellming R.M., Howell S.B.,
 Kreidl T.J., 1994, ApJ, 429, 125
 Zurita C., Casares J., 1998, in J. Paul, T. Montmerle, and
 E. Aubourg eds., Abstracts of the 19th Texas Symposium
 on Relativistic Astrophysics and Cosmology, Paris
 Zurita C., Casares J., Shahbaz T., Wagner R.M., Foltz
 C.B., Rodríguez-Gil P., Hynes R.I., Charles P.A., Ryan
 E., Schwarz G., Starrfield S.G., 2002, MNRAS, 333, 791
 Zurita C., Casares J., Shahbaz T., 2003, ApJ, 582, 369

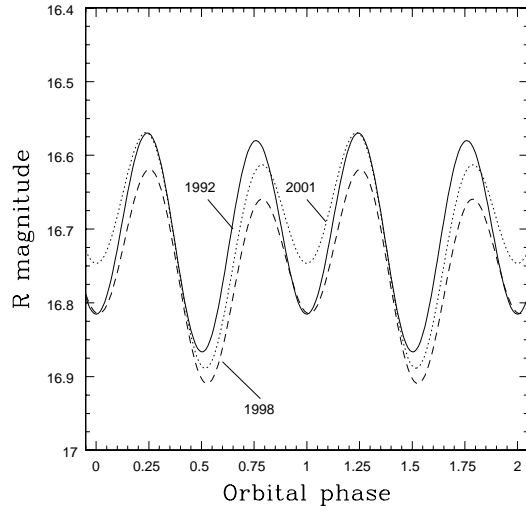


Figure 1. Ellipsoidal model fits to the lower envelopes of the 1992 (continuum line), 1998 (dashed line) and 2001 (pointed line) *R*-band lightcurves.

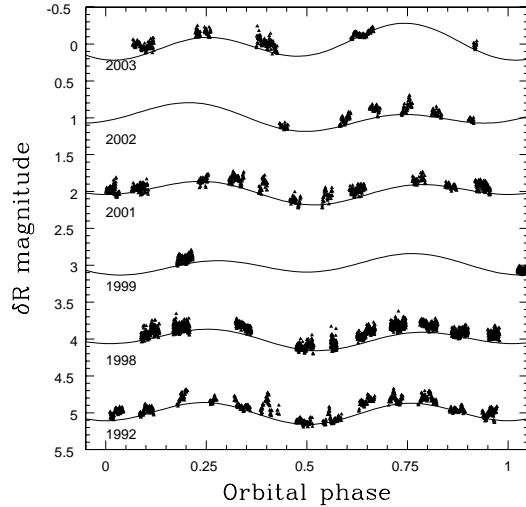


Figure 2. The *R* band ellipsoidal lightcurves of V404 Cyg for 1992, 1998, 1999, 2001, 2002 and 2003 and the lower envelopes constructed as explained in section 3. Different magnitude offsets were applied for clarity.

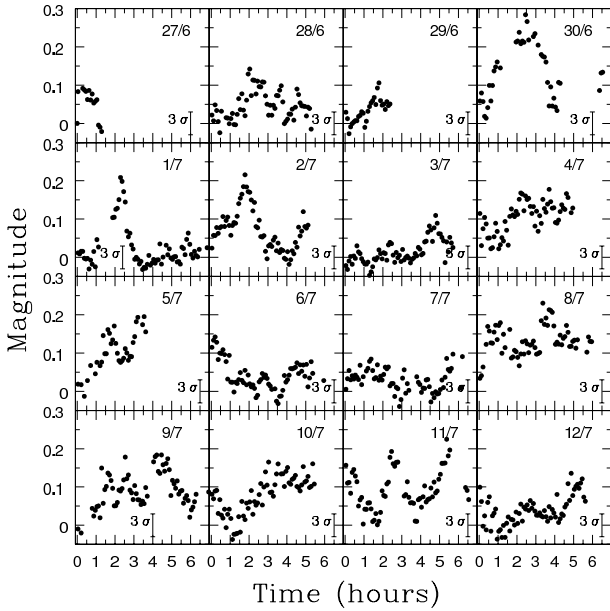


Figure 3. *R* band lightcurves of V404 Cyg after subtracting the ellipsoidal modulation – 1992 lightcurves.

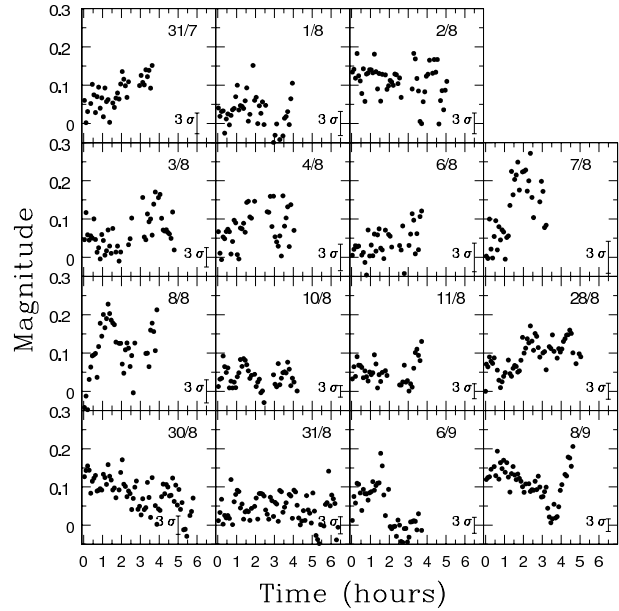


Figure 3. *R* band lightcurves of V404 Cyg after subtracting the ellipsoidal modulation – 2001 lightcurves.

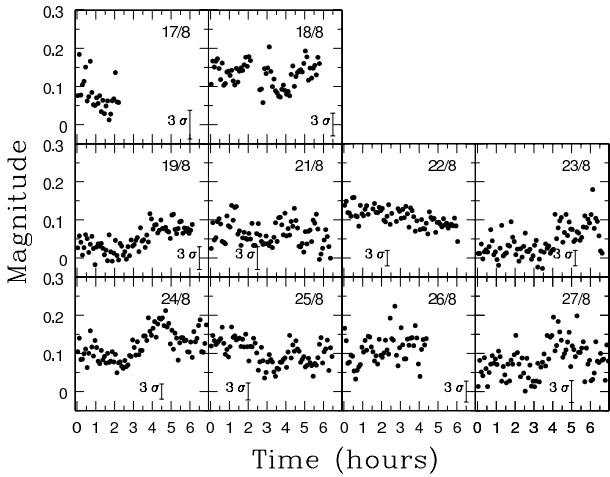


Figure 3. *R* band lightcurves of V404 Cyg after subtracting the ellipsoidal modulation – 1998 lightcurves.

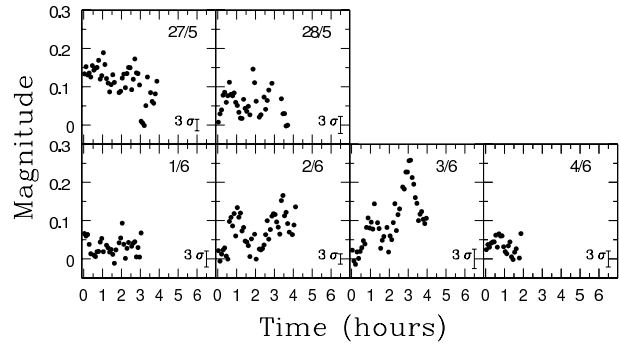


Figure 3. Continued – 2002 lightcurves.

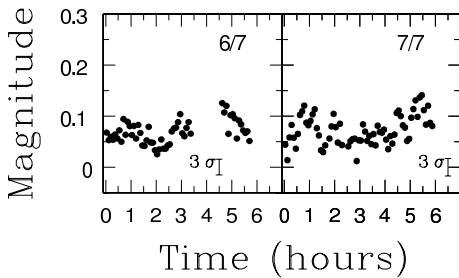


Figure 3. *R* band lightcurves of V404 Cyg after subtracting the ellipsoidal modulation – 1999 lightcurves.

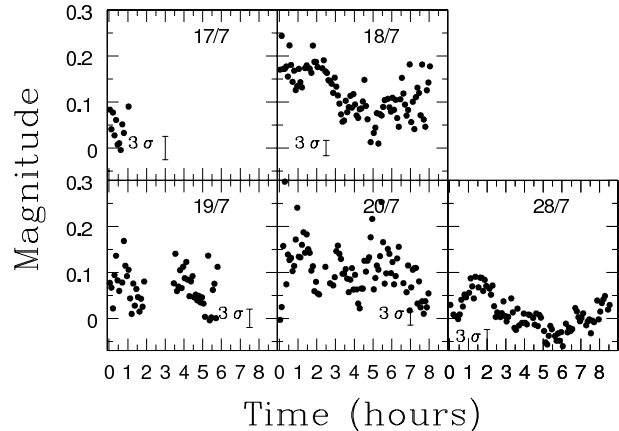


Figure 3. Continued – 2003 lightcurves.

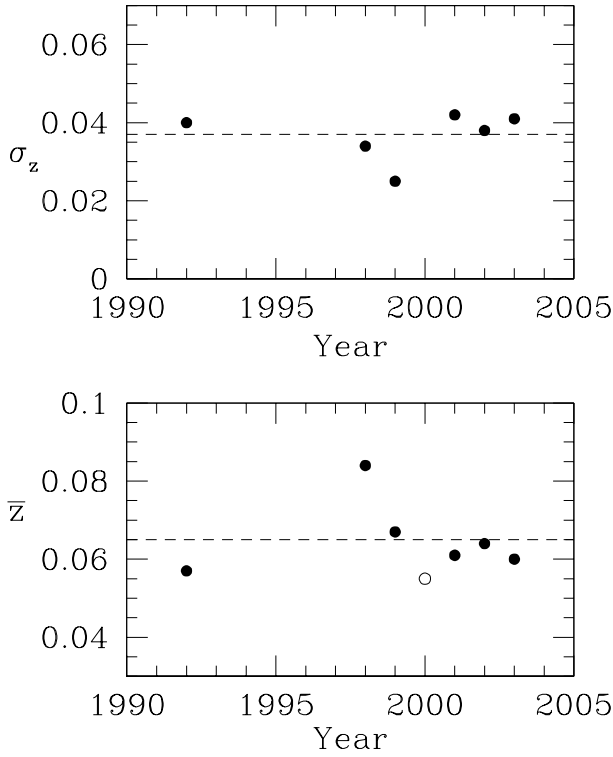


Figure 4. Mean relative intensity and flare activity over the last decade. Mean levels are marked by dashed lines. The open circle marks the value measured by Pavlenko et al. (2001).

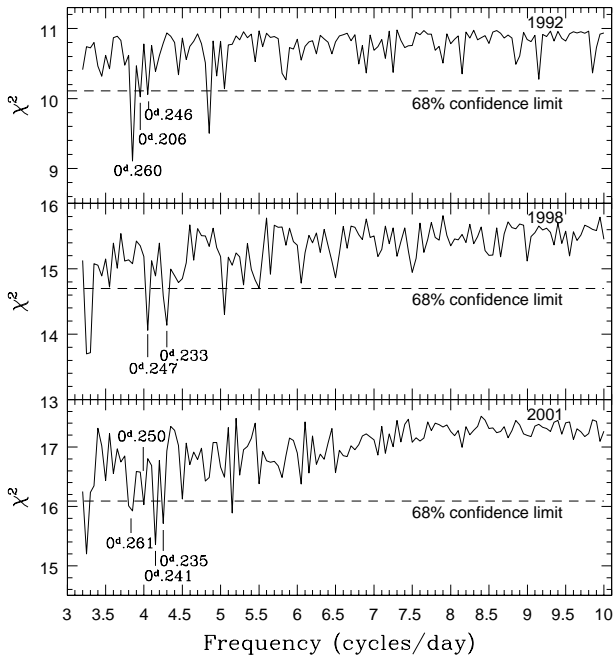


Figure 5. χ^2 minimization spectrum of the data after subtraction of the lower envelope. Dashed lines marks the 68 percent confidence limits at $\chi^2_{min} + 1$.

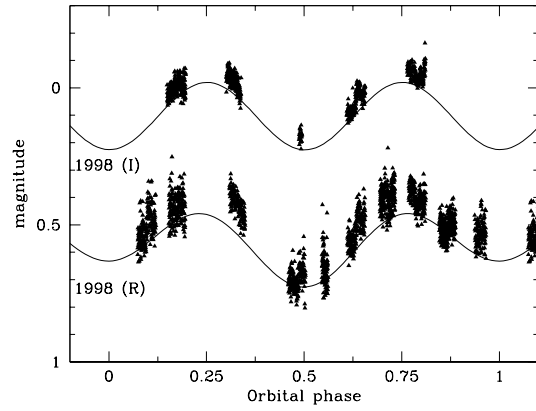


Figure 6. The *R* and *I* 1998 lightcurves and the lower envelopes constructed as explained in section 3.

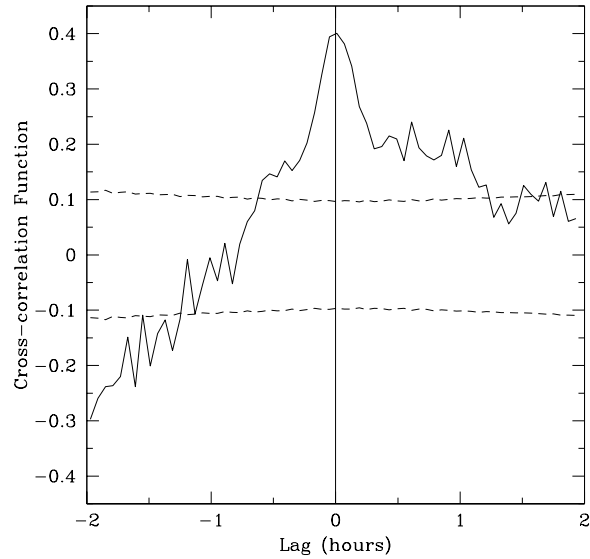


Figure 7. Cross-correlation function between *R* and *I* band data. A positive lag would correspond to *R* variations lagging behind those in *I*. Dotted lines indicate 3σ limits on expected coincidental correlations.

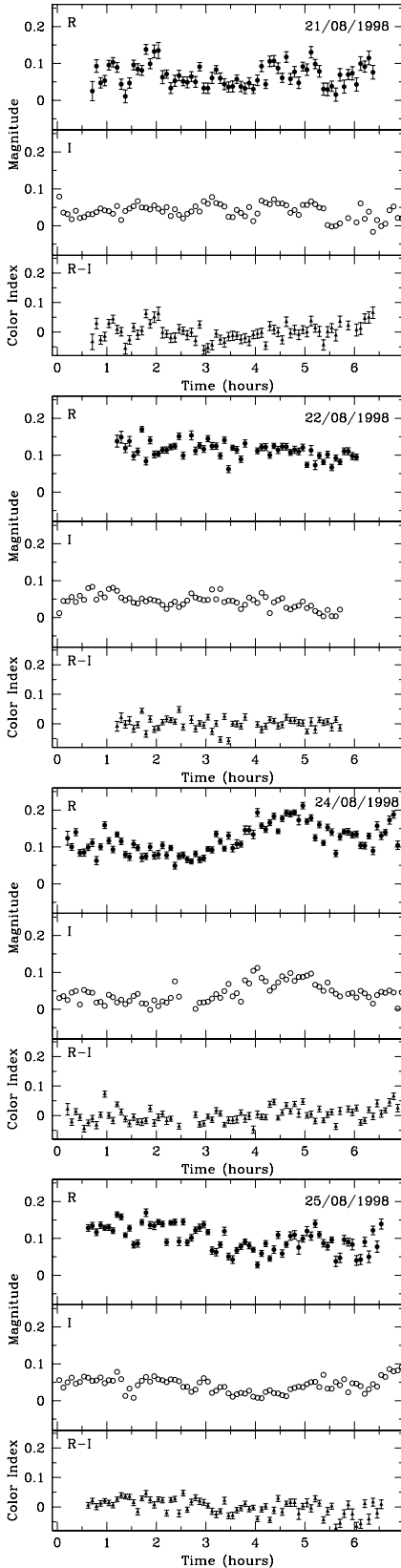


Figure 8. The 1998 *R*, *I* and color *R*–*I* lightcurves of V404 Cyg after subtracting the ellipsoidal modulation.

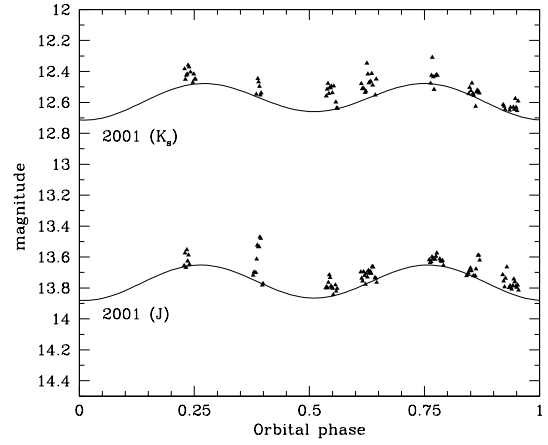


Figure 9. The *J* and *K_s* ellipsoidal 2001 lightcurves and the lower envelopes constructed as explained in section 3.

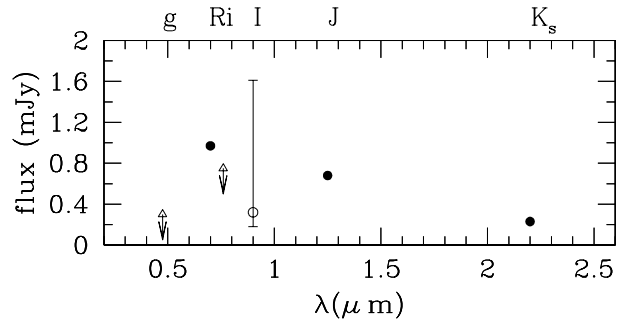


Figure 10. Mean flare flux densities in the *R*, *J* and *K_sshort* bands calculated with the 2001 data (close circles). The open circle is the expected *I* density flux assuming the ratio $F_R/F_I = 3$ obtained with the 1998 data. Triangles are the mean flare flux densities calculated by Shahbaz et al. (2003b) in the *g'* and *i'* bands ($\lambda_{eff} = 4750 \text{ \AA}$ and 7650 \AA respectively).

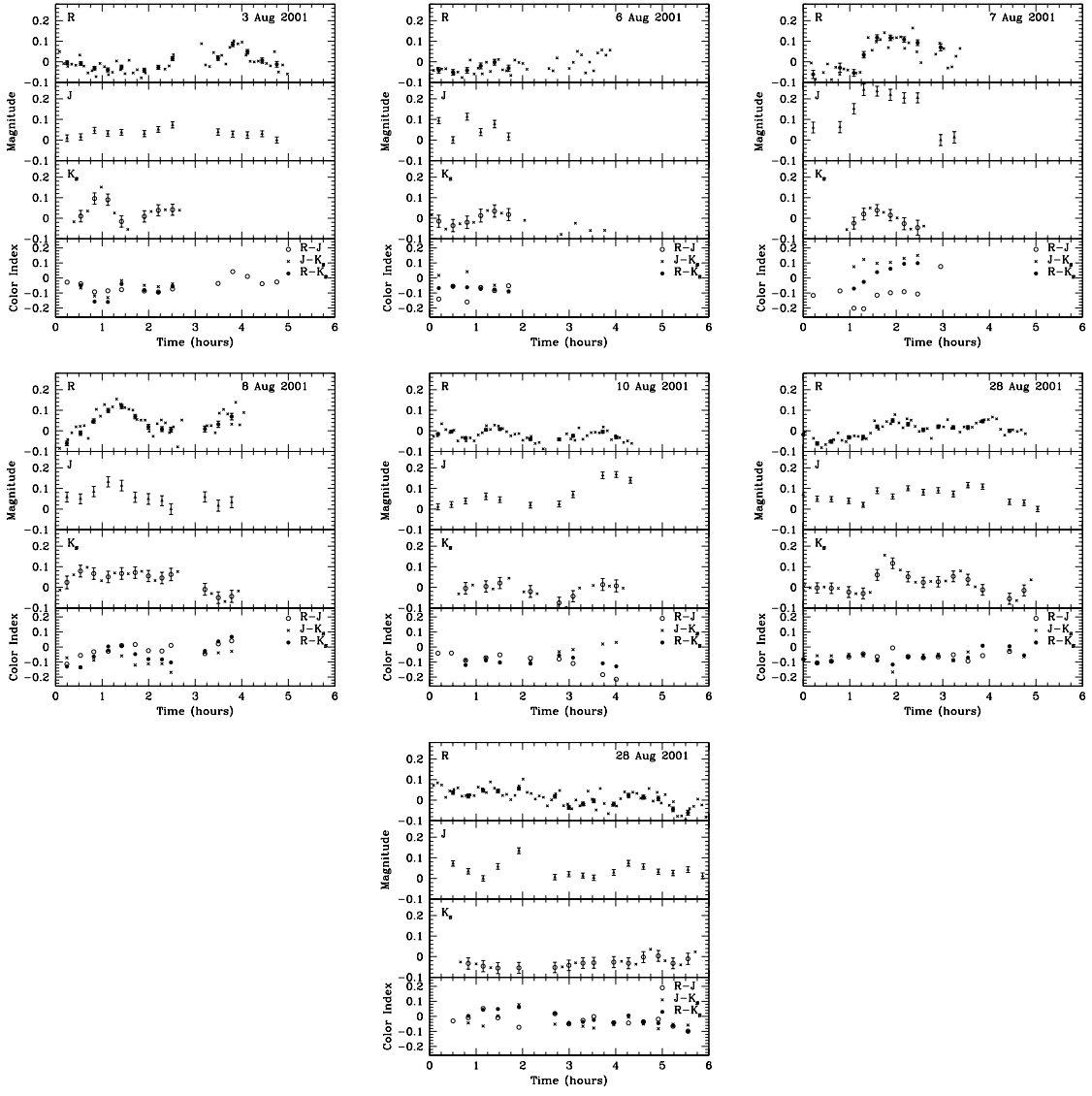


Figure 11. From top to bottom: The R , J and K_s lightcurves of V404 Cyg (after subtracting the ellipsoidal modulation) and the color indices $R - K_s$, $J - K_s$ and $R - J$. Crosses mark the original data and circles the new resampled data.

This paper has been typeset from a $\text{T}_{\text{E}}\text{X}/\text{L}^{\text{A}}\text{T}_{\text{E}}\text{X}$ file prepared by the author.